Journal of Orthopaedic Translation 38 (2023) 141–155

Contents lists available at ScienceDirect

Journal of Orthopaedic Translation

journal homepage: www.journals.elsevier.com/journal-of-orthopaedic-translation

Therapeutic effect of induced pluripotent stem cell -derived extracellular vesicles in an *in vitro* and *in vivo* osteoarthritis model

Yu-Huan Hsueh [a,b], Waradee Buddhakosai [b], Phung Ngan Le [b], Yung-Yi Tu [c], Hsien-Chang Huang [b], Huai-En Lu [d,e,*], Wen-Liang Chen [f,**], Yuan-Kun Tu [b,***]

[a] College of Biological Science and Technology, National Yang Ming Chiao Tung University, Hsinchu, Taiwan
[b] Department of Orthopedic Surgery, E-Da Hospitall, I-Shou University, Kaohsiung, Taiwan
[c] School of Medicine, National Taiwan University, Taipei, Taiwan
[d] Bioresource Collection and Research Center, Food Industry Research and Development Institute, Hsinchu City, Taiwan
[e] Institute of Biochemistry and Molecular Biology, National Yang Ming Chiao Tung University
[f] Department of Biological Science and Technology, National Yang Ming Chiao Tung University, Hsinchu, Taiwan

ARTICLE INFO

Keywords:
Extracellular vesicles
Inflammation
Macrophages
Osteoarthritis

ABSTRACT

Background/Objective: Osteoarthritis (OA) is a multifactorial joint disease associated with the deterioration of chondrocytes and inflammation. Treatment of OA is only aimed at reducing pain and improving joint function. Recently, extracellular vesicles (EVs) secreted from stem cells have emerged as a cell regenerative tool in several degenerative diseases, including OA. We hypothesised that induced pluripotent stem cell (iPSC)-derived EVs would be beneficial for regenerating chondrocytes and OA therapy. Therefore, we aimed to investigate iPSC-EVs' effects on chondrocyte behaviour in an interleukin 1 beta (IL-1β)-induced *in vitro* OA model and anterior cruciate ligament transection (ACLT)-induced *in vivo* OA model of rabbit articular cartilage.

Methods: The iPSC-EVs were isolated by sequential ultracentrifugation from a 48-h-incubated conditional medium of iPSC. The isolated iPSC-EVs were characterised by transmission electron microscopy, western blot analyses, and dynamic light scatter. The effects of iPSC-EVs on the viability of human primary chondrocytes and cell senescence were analysed. Premature senescence of cells was induced by long-term incubation with low doses of hydrogen peroxide. To investigate the therapeutic effect of iPSC-EVs on OA chondrocytes *in vitro*, IL-1β was used to induce chondrocyte damage. Inflammatory macrophages were activated from THP-1 monocytes to observe the impact of iPSC-EV on macrophage polarisation. The phenotypes of the macrophages exposed to iPSC-EVs were evaluated by ELISA and western blot analyses. The primary chondrocytes were co-cultured with different phenotypes of macrophages to observe the expression of collagen II and catabolic enzymes in chondrocytes. iPSC-EVs were injected intraarticularly into the rabbit with an ACLT-induced OA model. The progression of lesions was assessed through macroscopic and histopathological studies.

Results: We showed that iPSC-EVs significantly stimulated the proliferation of primary human chondrocytes and suppressed cell senescence by regulating the expression of p21 and collagen II. iPSC-EVs reduced matrix degradation enzymes and IL-6 expression and attenuated IL-1β-mediated cell death of chondrocytes. Furthermore, iPSC-EVs modulated macrophage polarisation, resulting in the rescue of damaged chondrocytes in an inflammatory microenvironment. In the rabbit ACLT model, the OA-like lesions, including inflammation, subchondral bone protrusion, and articular cartilage destruction, were ameliorated by iPSC-EV. A histopathological study consistently revealed that iPSC-EVs attenuated ACLT-mediated alteration of MMP13 and ADAMTS5 and collagen II expression.

Conclusion: iPSC-EVs protected chondrocytes by enhancing cell proliferation, suppressing premature senescence, and maintaining homeostasis of collagen II synthesis and matrix degradation enzymes such as matrix metalloproteinases (MMPs) and ADAMTS5. iPSC-EVs also reduced cell death in IL-1β-mediated chondrocyte cell damage. In the rabbit ACLT-induced OA model, iPSC-EV injection reduced cartilage destruction, as indicated by

* Corresponding author. Institute of Biochemistry and Molecular Biology, National Yang Ming Chiao Tung University, Hsinchu, Taiwan.
** Corresponding author.
*** Corresponding author.
E-mail addresses: Oscar9272000@hotmail.com (Y.-H. Hsueh), saimunor@gmail.com (W. Buddhakosai), vanialai.yin@gmail.com (P.N. Le), bobby890208@gmail.com (Y.-Y. Tu), luckylogo0529@gmail.com (H.-C. Huang), hel@firdi.org.tw (H.-E. Lu), wenurea@yahoo.com.tw (W.-L. Chen), ed100130@edah.org.tw (Y.-K. Tu).

https://doi.org/10.1016/j.jot.2022.10.004
Received 5 January 2022; Received in revised form 16 August 2022; Accepted 7 October 2022

2214-031X/© 2022 Published by Elsevier B.V. on behalf of Chinese Speaking Orthopaedic Society. This is an open access article under the CC BY-NC-ND license (http://creativecommons.org/licenses/by-nc-nd/4.0/).

the upregulation of collagen II and down-regulation of MMP13 and ADAMTS5. Overall, our results suggest that iPSC-EVs possess therapeutic potential and may be used as an OA treatment option.
The translational potential of this article: This study highlights the potential of iPSC-EVs as a therapeutic option for chondrocyte regeneration and OA treatment.

1. Introduction

Osteoarthritis (OA) is one of the most common age-related arthritis and can affect multiple synovial joints. The knee is the most common site of OA, accounting for 16% of the global prevalence [1]. OA is caused by multifactorial aetiologies such as age, obesity, genetics, gender/hormone status, and trauma [2]. OA is a complex process involving the entire joint apparatus, characterised by degeneration or fissure formation in the cartilage, matrix fibrillation, synovial inflammation, osteophyte formation, and subchondral bone sclerosis [3,4]. The pathogenesis of OA is related to the altered proliferation, apoptosis, and behaviour of chondrocytes, including aberrant production of cartilage-degrading enzymes and hypertrophy markers. As a result, the extracellular matrix (ECM) surrounding the chondrocytes is usually damaged. Low-grade inflammation is present in OA, including the release of cytokines such as interleukin 1 beta (IL-1β), IL-6, interferon-gamma (IFN-γ), and tumour necrosis factor-alpha (TNFα) from inflammatory synovial tissues [5]. These cytokines and other mediators stimulate abnormalities in chondrocytes, such as anabolic-catabolic homeostasis imbalance, excessive catabolic enzyme expression, senescence, and apoptosis, leading to degeneration of the ECM.

Current OA treatment is directed toward supportive therapy to reduce pain, improve joint mobility, and limit disease progression [6]. The primary strategy of OA management is based on drugs and regenerative medicine, such as cell transplantation [7]. Several drugs have been used to target the catabolic-anabolic pathway of chondrocytes or inflammatory processes. Stem cells are used to regenerate defective cells. Mesenchymal stem cells (MSCs) derived from bone marrow [8] and adipose tissue [9] were grafted in patients with OA with promising results in pain management and functional recovery. Recently, accumulating evidence has demonstrated that the therapeutic potential of cell transplantation is mediated by the paracrine effect of the secretome, a mixture of soluble factors and extracellular vesicles (EVs) secreted from transplanted cells [10].

EVs are complex membrane-bound transporter organelles secreted by cells into the extracellular environment, mediating communication between cells. Recent studies have revealed that EVs isolated from stem cells have therapeutic effects on OA. EVs produced by embryonic stem cell-derived mesenchymal stem cells (ESC-MSCs) alleviate IL-1β-mediated cell damage of chondrocytes by inducing collagen II synthesis and reducing ADAMTS5 expression. Furthermore, intra-articular injection of ESC-MSC EVs has ameliorated cartilage degeneration and matrix degradation in the destabilisation of the medial meniscus-induced OA in mice [11]. EVs derived from human bone marrow stem cells (hBMSCs) promote cell proliferation and inhibit apoptosis in human OA chondrocytes and IL-1β-mediated OA chondrocytes [12]. Induced pluripotent stem cell (iPSCs) can be derived from various sources, including peripheral blood mononuclear cells (PBMC) [13], and although culture of iPSCs is more complex, previous reports have demonstrated that iPSCs produce 16-fold more EVs than MSCs [14]. In addition, EVs derived from human iPSC (iPSC-EVs) can restore collagen I expression and reduce fibroblast expression of matrix metalloproteinases (MMPs)-1/-3, catabolic enzymes related to ECM degradation and OA pathogenesis. However, little is known about iPSC-EVs' effect in chondrocytes and OA models.

This study aimed to investigate the effect of iPSC-EVs on chondrocyte behaviour in an IL-1β-induced *in vitro* OA model and anterior cruciate ligament transection (ACLT)-induced *in vivo* rabbit articular cartilage OA model. We hypothesised that iPSC-EVs play a role in the macrophage microenvironment involved in inflammation.

2. Materials and methods

2.1. hiPSC lines and maintenance

The hiPSCs were provided by Dr Lu, Bioresource Collection and Research Center (BCRC), Food Industry Research and Development Institute, Hsinchu, Taiwan. Characterisation and validation results are on the BCRC website: https://catalog.bcrc.firdi.org.tw/. Briefly, hiPSC lines were generated from human PBMCs using the CytoTune iPS 2.0 Sendai Reprogramming Kit protocol (Invitrogen) and were used according to the Policy Instructions of the Ethics of Human Embryo and Embryonic Stem Cell Research guidelines in Taiwan. The hiPSCs were maintained in StemFlex medium (Gibco) on Matrigel-coated dishes following the manufacturer's instructions.

2.2. iPSC-EV isolation and characterisation

The iPSC-EVs were isolated by sequential ultracentrifugation. Briefly, the iPSCs were cultured in a serum-free medium (6 mL/6 cm^2 dish) for 48 h. The iPSC conditional medium was then transferred into 50-mL centrifuge tubes and centrifuged at 300×*g* for 5 min. The supernatant was transferred to a new tube and centrifuged at 2,000×*g* for 30 min, then transferred and centrifuged at 10,000×*g* for 30 min. The supernatant was then transferred to an ultracentrifuge tube and centrifuged at 100,000×*g* for 70 min to pellet the EV. The supernatant was discarded, and the EV pellet was washed in phosphate-buffered saline (PBS) and centrifuged at 100,000×*g* for 70 min. All centrifugation steps were performed at 4 °C. The isolated EVs were resuspended in PBS for characterisation and subsequent treatment. A lysis buffer was added directly to the EV pellet for western blot analysis of the EV surface markers. The concentration of the EVs was measured using a bicinchoninic acid (BCA) assay (Pierce BCA protein assay, Invitrogen). EV samples were immediately used, or stored at −20 °C or −80 °C for two weeks or longer, respectively. Isolated iPSC-EV morphology was characterised using a transmission electron microscope (TEM; Hitachi HT7700 (100 kV)). Nanovesicle size distribution was analysed using dynamic light scattering (DLS). MA-tek Material Analysis Technology Inc performed TEM and DLS analyses.

2.3. 1,1′-dioctadecyl-3,3,3′,3′-Tetramethylindocarbocyanine Perchlorate labelling

Isolated iPSC-EVs were labelled with 1,1′-Dioctadecyl-3,3,3′,3′-Tetramethylindocarbocyanine Perchlorate (DiI). Briefly, DiI was dissolved, filtered, and added to EV samples to a final concentration of 6 μM. Labelled EV samples were then gently shaken at room temperature for 1 h.

2.4. Primary chondrocyte culture

Articular cartilage was collected from the femoral condyle of patients (n = 6) under sterile conditions after obtaining written consent from each patient, approved by the IRB committee of E-da Hospital, Taiwan (IRB number: EMRP-108-008). Patient age ranged from 21 to 78 years. The harvested cartilage surface was smooth, slippery, and white, without fissures or erosions. The surgically collected tissue was transferred into a 50 mL centrifuge tube containing sterile PBS at 4 °C. The cartilage was transferred to a Petri dish containing DMEM/F12 (Invitrogen) culture medium with 1% penicillin-streptomycin and then cut using a sterile

surgical blade. The divided cartilage was then transferred to a T25 flask containing 1 mg/mL of Pronase (Roche) in DMEM/F12 with 1% penicillin-streptomycin and incubated at 37 °C with 5% CO_2 for 30 min. After discarding the enzyme solution and washing in PBS +1% penicillin-streptomycin, the tissue was digested overnight in 1 mg/mL collagenase (Invitrogen) at 37 °C with 5% CO_2. The cell suspension was then transferred to a 50 mL centrifuge tube and centrifuged at 300×*g* for 5 min. The supernatant was decanted, and the cell pellet was washed in PBS and centrifuged at 300×*g* for 5 min. The supernatant was discarded. The cell pellet was re-suspended in a conventional medium containing DMEM/F12 + 1% penicillin-streptomycin and 10% foetal bovine serum (FBS) and seeded in a flask to expand in two-dimensional culture (passage 0).

2.5. Western blot

To harvest the total protein, lysis buffer containing Pierce™ RIPA buffer (Invitrogen) with 1x protease inhibitor (Halt™ Protease and Phosphatase Inhibitor cocktail, Invitrogen) was applied to the cells or EV pellet. The sample was vortexed and centrifuged at 13,000×*g* for 10 min. The supernatant containing the protein was transferred into a new tube. The protein concentration was quantified using a BCA kit (Pierce BCA protein assay, Invitrogen). Fifteen micrograms of each protein sample were loaded onto each well of the SDS-PAGE. After electrophoresis, the proteins on the SDS-PAGE were transferred onto a polyvinylidene difluoride (PVDF) membrane. The PVDF membrane was blocked in 5% skim milk in Tris-buffered saline +0.1% Tween-20 (TBST) for 1 h at room temperature, followed by incubation with primary antibodies at 4 °C overnight. The membrane was washed three times with TBST and incubated with horseradish peroxidase-conjugated secondary antibodies for 1 h at room temperature with gentle shaking. Subsequently, immunoreaction was detected using an enhanced chemiluminescence reagent according to the manufacturer's instructions (Millipore). The primary antibodies used in this study were as follows: from GeneTex, Inc. at 1:1000, CD9 (GTX66709), CD81 (GTX31381), TSG101 (GTX70255), p21 (GTX629543), MMP13 (GTX100665), ADAMTS5 (GTX100332), iNOS (GTX60599), and TNF-α (GTX110520), at 1:1500, IL-6 (GTX110527), and at 1:3000, beta-actin (GTX109639); from System Biosciences, Inc. at 1:1000, CD63 (EXOAB-CD63A-1); and from Abcam at 1:1000, Collagen II (ab185430) and CD206 (ab125028).

2.6. Cell proliferation assay

Primary chondrocytes in passages 2–5 (10^5 cells/mL) were inoculated into 96-well plates and cultured in the conventional medium described above. iPSC-EV was added to the treatment group at a final concentration of 10 μg/mL medium (with 1% FBS). An equal volume of PBS was added to the control group. The cells were incubated for three days and counted for proliferation analysis using the Cell Counting Kit-8 (CCK-8, Dojindo Molecular Technology, Japan). On day 3, CCK-8 solution was added to the wells, and the plates were incubated at 37 °C for 2 h. Absorbance was measured at 450 nm using a microplate reader (BioTek 800 TS, Agilent).

2.7. H_2O_2-induced senescence and senescence-associated β-galactosidase cell staining (SA-β-gal staining)

Primary chondrocytes in passages 2–3 (10^5 cells/mL) were seeded into 6 cm^2 culture dishes and cultured in DMEM/F12 medium (supplemented with 10% FBS and 1% penicillin-streptomycin). From day 3, H_2O_2 was applied to the cells at a final concentration of 10 μM for four consecutive days. On day 7, the cells were sub-passaged, and the protocol was repeated for two more cycles. Next, the control cells were cultured and sub-passaged along with senescent chondrocytes without H_2O_2 treatment. To begin the last cycle, control and H_2O_2-treated cells were sub-passaged into 6 cm^2 dishes for western blot analysis or 48-well plates for SA-β-galactosidase staining. In this cycle, control and H_2O_2-treated cells were divided into two groups (iPSC-EV- or iPSC-EV+). On day 7 of the last passage (day 22 of the experiment), the medium was changed to a 1% FBS medium with or without 10 μg/mL iPSC-EV, and the cells were incubated for three days. The cells were harvested and put in a lysis buffer for protein isolation and western blot analysis. SA-β-galactosidase staining was performed using the SA-β-galactosidase staining kit (#9680, Cell Signalling Technology) following the manufacturer's instructions. Briefly, in a 48-well plate, the medium was discarded, and the cells were rinsed once in PBS. The cells were then fixed in a fixative reagent for 10 min. After three washes in PBS, the cells were incubated overnight in the β-galactosidase staining solution at 37 °C without CO_2. The cells were observed using a microscope (Olympus CKX53).

2.8. IL-1β stimulation of OA chondrocytes and iPSC-EV treatment

Chondrocytes in passages 2–5 (10^5 cells/mL) were plated in 6 cm^2 culture dishes and maintained in the culture medium described above. When the cells reached 80% confluency, the medium was replaced with fresh medium (1% FBS) containing recombinant human IL-1β protein (ab9617, Abcam) at 10 ng/mL to induce OA chondrocytes or at 20 ng/mL to induce cell death (for live-dead cell imaging). iPSC-EV was applied along with IL-1β treatment at a final concentration of 10 μg/mL [15,16], and the cells were incubated for 24 h.

2.9. Live-dead cell analysis

After 24 h of treatment with 20 ng/mL IL-1β with or without iPSC-EV, the medium was discarded. The cells were rinsed in dPBS once before incubation in 5x Live and Dead Dye (ab115347, Abcam) for 10 min at room temperature with gentle shaking. The number of live and dead cells was determined using a fluorescent microscope (Olympus CKX53). The number of red fluorescent cells (dead) was quantified as a percentage of the total population.

2.10. ELISA

The macrophage-conditioned media (CM) were collected and centrifuged at 300×*g* for 5 min to quantify the level of cytokines secreted by macrophages. The supernatant was collected in a new tube and used for ELISA. Human IL-1β ELISA kit (ab46052, Abcam), Human TNF-α ELISA kit (KHC3011, Invitrogen), and Human IL-6 ELISA kit (KHC0061) were used in this study, following manufacturers' instructions.

2.11. Macrophage polarisation

THP-1 monocytes (passage 20–23) were cultured in RPMI 1640 (A1049101, Gibco) supplemented with 1% penicillin-streptomycin and 5% FBS. To activate the THP-1 monocytes to naïve macrophages (M0), 50 ng/mL of phorbol 12-myristate 13-acetate (PMA) (P8139, Sigma–Aldrich) was added to the cells (10^6 cell/mL) and incubated for 24 h. The cells were then rested in fresh medium for 24 h before polarisation to pro-inflammatory macrophages (M1). For polarisation, the cells were incubated in a medium containing 20 ng/mL IFN-γ and 500 ng/mL lipopolysaccharide (LPS) for 24 h. Then cells were collected for protein extraction and western blot analysis. To harvest macrophage-CM for the treatment of chondrocytes, the medium was refreshed and incubated for one more day before harvesting.

2.12. MMP array

The CMs of the different macrophages (M0, M0 + iPSC-EV, M1, and M1 + iPSC-EV) were collected and centrifuged at 300×*g* for 5 min to remove cell debris. These collected CMs were then applied to the chondrocytes at 50% concentration (1:1 chondrocyte medium with 5% FBS: macrophage-CM). Chondrocytes were incubated in the media for 24 h. The control group was cultured in a 100% conventional chondrocyte medium. The medium was replaced with fresh serum-free medium and

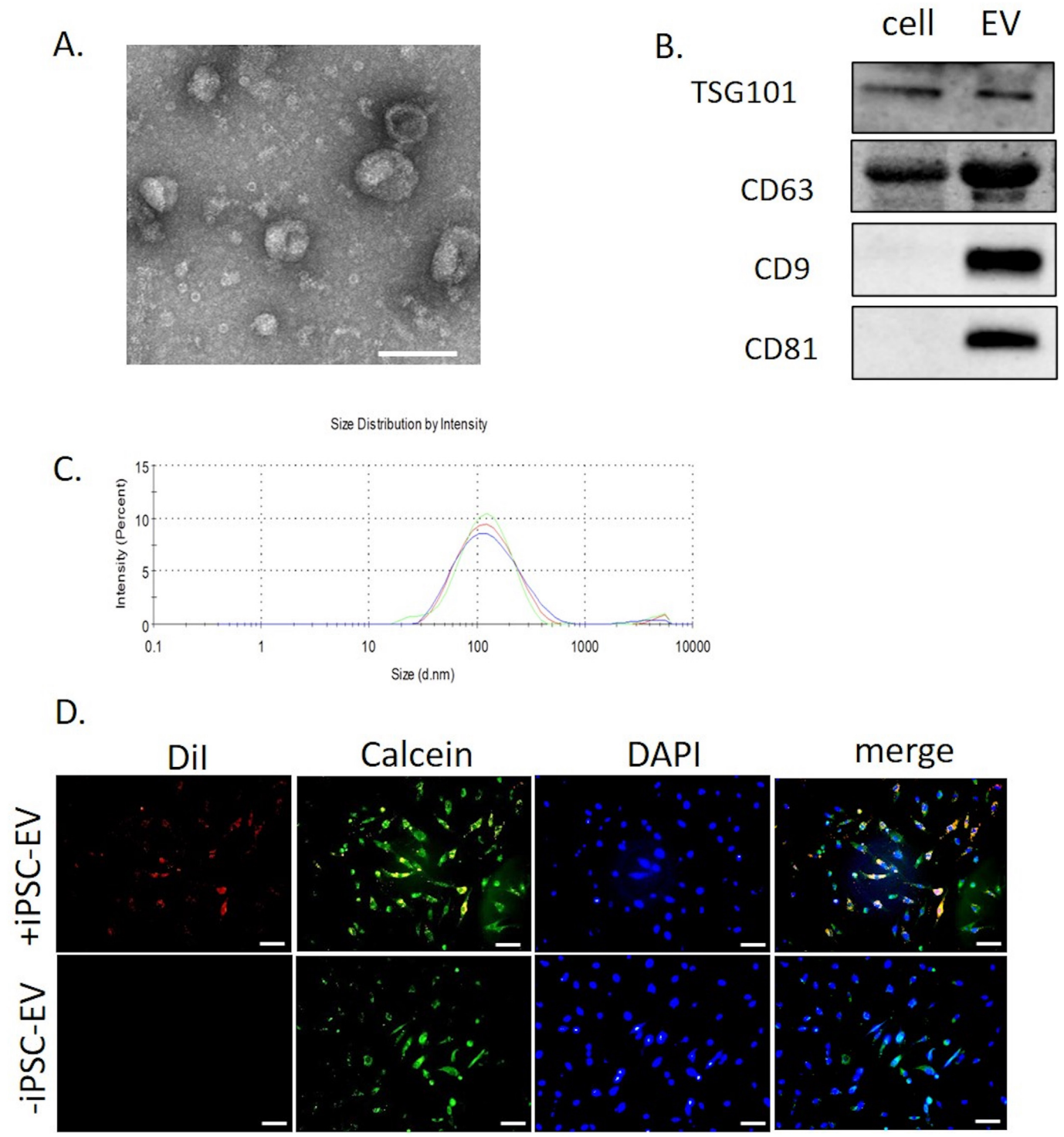

Figure 1. iPSC-derived EV characterisation. A. TEM image demonstrates the cup-shaped particles of iPSC-EVs., scale bar = 100 nm. B. A representative western blot image showing EV surface markers (TSG101, CD63, CD9, and CD81). C. Particle size distribution of iPSC-EVs measured by DLS method. D. Internalisation of iPSC-EV in primary human chondrocyte was visualised under the fluorescent microscope. iPSC-EV was labelled with DiI (red). Calcein (green) and DAPI (blue) were used to stain the cell body and chondrocyte nuclei, respectively. Scale bar = 200 μm. (For interpretation of the references to colour in this figure legend, the reader is referred to the Web version of this article.)

Abbreviations: EVs: Extracellular vesicles; DLS: dynamic light scattering; iPSC: induced pluripotent stem cell; iPSC-EV: induced pluripotent stem cell-derived extracellular vesicles

each group was cultured for an additional 24 h. The CMs of the chondrocytes (five groups) were harvested for MMP array analysis. A human MMP antibody array membrane (ab134004, Abcam) was used, following the manufacturer's instructions. Chondrocyte cell samples were harvested for total protein isolation and western blot analysis.

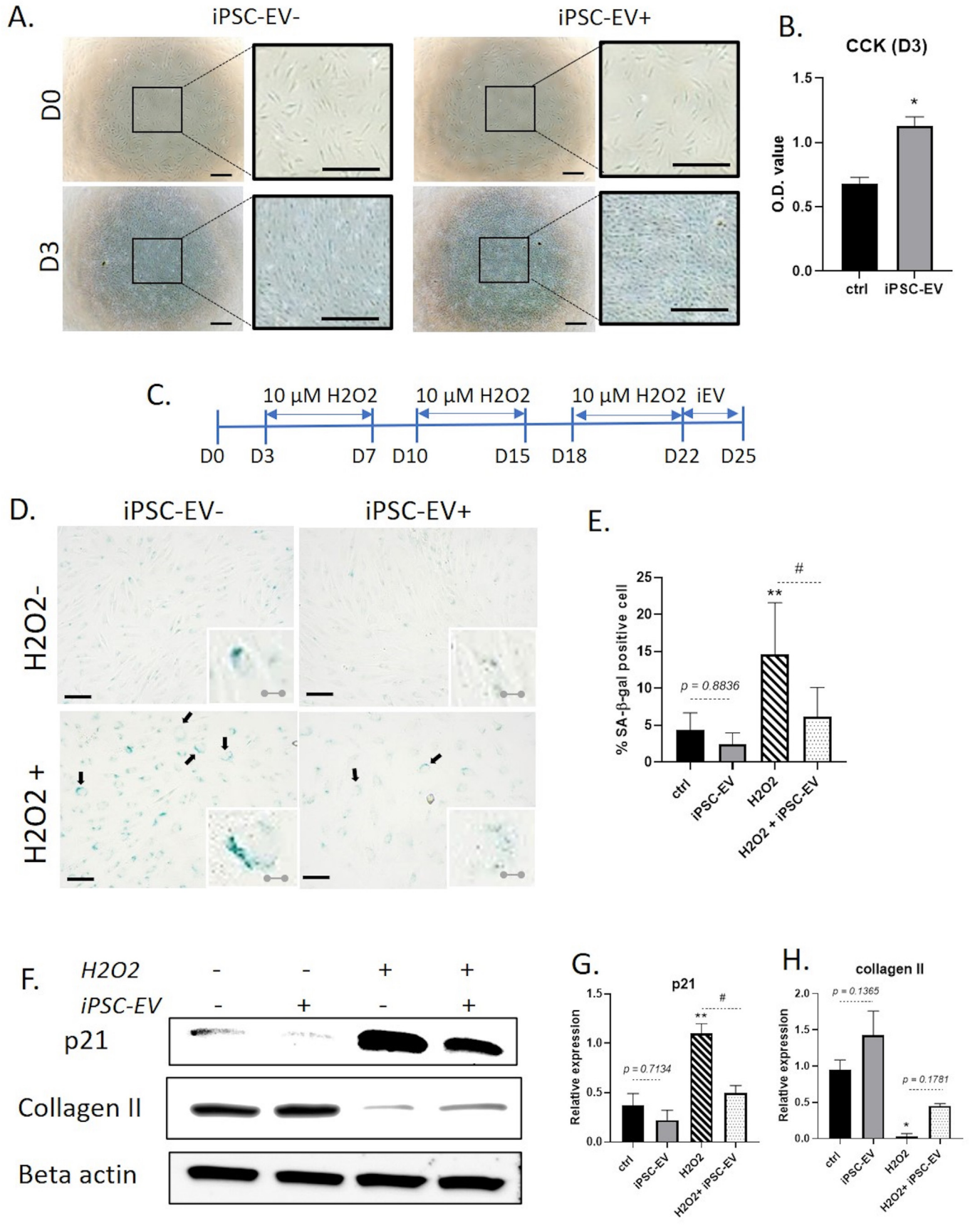

(caption on next page)

Figure 2. iPSC-EV enhanced proliferation and inhibition of senescence of primary human chondrocytes. A. Phase-contrast image of chondrocyte culture in normal and iPSC-EV supplemented condition. Scale bar 500 μm. B. The graph shows chondrocyte cell proliferation assessed using a CCK8 assay (n = 4) C. A schematic protocol of H_2O_2-induced senescence of chondrocytes. D. SA-β-galactosidase staining of chondrocytes. Scale bar = 100 μm. A small box on the bottom right of each image shows the expansion of positively stained cells. Scale bar = 20 μm. Black arrows indicate irregular cells. E. Quantitation of SA-β-galactosidase positive cell (n = 5) F. Representative western blot image demonstrating the expression levels of senescence markers p21 and collagen type II in chondrocytes from different treatments. G., H. Densitometry of p21, and collagen II, respectively (n = 3) *Significant difference to control: *p < 0.05; **p < 0.01. # Significant difference between groups: #p < 0.05.
Abbreviations: iPSC-EV: induced pluripotent stem cell-derived extracellular vesicles; CCK-8: Cell Counting Kit-8; H2O2: hydrogen peroxide; SA-β-galactosidase: senescence associated -β-galactosidase

2.13. Macrophage-chondrocyte co-culture and immunocytochemistry

THP-1 cells (passage 20–24), at a concentration of 10^6 cells/mL, were inoculated into the upper inserts of 24-well Transwell plates. Macrophage activation and polarisation were performed as described previously. After polarisation, the upper inserts were transferred to the wells where chondrocytes (passages 2–3) were cultured (10^5 cells/mL) in complete medium with 10% FBS. Macrophages and chondrocytes were co-cultured for 24 h. The upper inserts were then removed. The cells were rinsed before fixation in 4% paraformaldehyde for 10 min and then washed three times. Non-specific binding was blocked using a blocking and permeabilizing solution (2% BSA + 5% FBS + 0.01% Triton-X in PBS). The cells were incubated with primary antibodies against MMP13 (1:250) and collagen II (1:500) overnight at 4 °C. The primary antibody mixtures were removed, and the cells were washed three times with a washing solution (1% BSA in PBS). The secondary antibody mixture (Alexa Fluor® 488 [AB150081, Abcam] 1:700 + Alexa Fluor® 594 [AB150116, Abcam] 1:700 in washing solution) was applied to the cells and incubated at room temperature for 1 h (in the dark), with gentle shaking. The nuclei were counterstained with a mounting medium containing DAPI (ab104139, Abcam). The fluorescence signal was observed and imaged using a fluorescence microscope (Olympus CKX53). Fluorescence intensity from fluorescence images was quantified in the ImageJ program. The correct total cell fluorescence (CTCF) was calculated as follows:

CTCF = integrated density – (area of selected cell x mean fluorescence of background).

2.14. In vivo OA model in rabbits

Nine healthy female New Zealand white rabbits weighing approximately 4000 g each were randomly divided into three experimental groups (n = 3 per group). The first and second groups (ACLT and ACLT + iPSC-EV) were subjected to ACLT at their right knee joints to induce knee OA. The left knee of each rabbit was considered a control. The rabbits were anaesthetised using isoflurane inhalation. A vertical midline incision was made on the skin over the right distal patella using a sterile surgical blade. The knee joint capsule was opened. A complete transection of the ACL was performed using sterile surgical scissors and a blade. The surgical site was then sutured. The third experimental group was the sham group, in which the rabbits underwent similar open surgery without ACL transection. After surgery, antibiotics, cefazolin (20 mg/kg) and tramadol hydrochloride (2 mg/kg) were injected into all rabbits daily for three consecutive days. The animals were monitored daily. At the third week post-operation, 100 μg iPSC-EV was injected intra-articularly to the right knee joint of the ACLT + iPSC-EV and sham groups. An equal volume of PBS was injected into the right knee joint of each rabbit in the ACLT group. The iPSC-EV injection was repeated once every week for three weeks. At six weeks post-operation, all rabbits were euthanised. The knee joints were opened to observe the gross lesion before sample collection for tissue preparation. The knee joints were preserved in 10% buffered formalin solution and decalcified in 10% ethylenediaminetetraacetic acid. The tissues were embedded in paraffin blocks and sliced to a thickness of 6 μm.

2.15. HE, toluidine blue, and Safranin-O staining

The sections were deparaffinized by incubation in an oven at 60 °C for 1 h and then in xylene twice for 10 min each. The slides were rehydrated in the following reagents: 100% ethanol twice for 5 min each, 95% ethanol for 5 min, 75% ethanol for 5 min, 50% ethanol for 5 min, and rinsed using tap water. The sections were stained with HE, toluidine, and safranin-O, as described previously [17].

2.16. Immunohistochemistry (IHC)

After deparaffinization and rehydration, the sections were incubated in 1 mg/mL pronase (ROC-10165921001, Roche®) for 30 min at 37 °C. After washing twice in PBST (PBS + 0.05% Tween-20), 5 mg/mL hyaluronidase (H3506, Sigma–Aldrich®) was applied to the sections and incubated for 30 min at 37 °C. IHC staining was performed using the mouse and rabbit-specific HRP/DAB (ABC) Detection IHC kit (ab64264, Abcam), following the manufacturer's instructions. Primary antibodies used for IHC were as follows: from GeneTex, Inc. at 1:200, MMP13 (GTX100665) and ADAMTS5 (GTX100332), and at 1:250, TNF-α (GTX110520); and from Abcam at 1:250, Collagen II (ab185430.

2.17. Statistical analyses

GraphPad Prism software 8.0.1 was employed for statistical analysis. The comparison between two groups was performed using an unpaired, two-tailed Student's *t*-test. The comparisons involving three or more experimental groups were performed using one-way analyses of variance (ANOVA) with Tukey multiple comparisons. The data are expressed as mean ± standard error of the mean (SEM). $p < 0.05$ was considered statistically significant.

3. Results

3.1. iPSC-EV isolation and characterisation

Once the iPSCs reached 70% confluency, the CM of iPSCs was harvested every two days for EV isolation. The average EV concentration was 0.284 μg/μL. The iPSC-derived EVs (iPSC-EVs) were morphologically characterised by TEM. TEM images showed cup-shaped nanoparticles, a typical EV characteristic (Fig. 1A). The expression of EV surface proteins, such as TSG101, CD9, CD63, and CD81, was detected by western blot analysis (Fig. 1B). DLS indicated that the average size of EV was 136.8 nm (Fig. 1C). The iPSC-EVs were labelled with DiI to observe cell uptake ability. Fig. 1D shows red fluorescence localised in the cytoplasm of chondrocytes, suggesting that DiI-labelled iPSC-EVs were internalised by the chondrocytes.

3.2. iPSC-EV enhanced proliferation rate and reduced senescence of chondrocyte

We first investigated the effect of iPSC-EVs on chondrocyte viability. Human primary chondrocytes were incubated in the culture medium supplemented with iPSC-EVs for 24 h. Fig. 2A shows that chondrocytes exposed to iPSC-EVs had a larger number of cells than the untreated control. Cell viability was evaluated using the CCK-8 method. The CCK-8

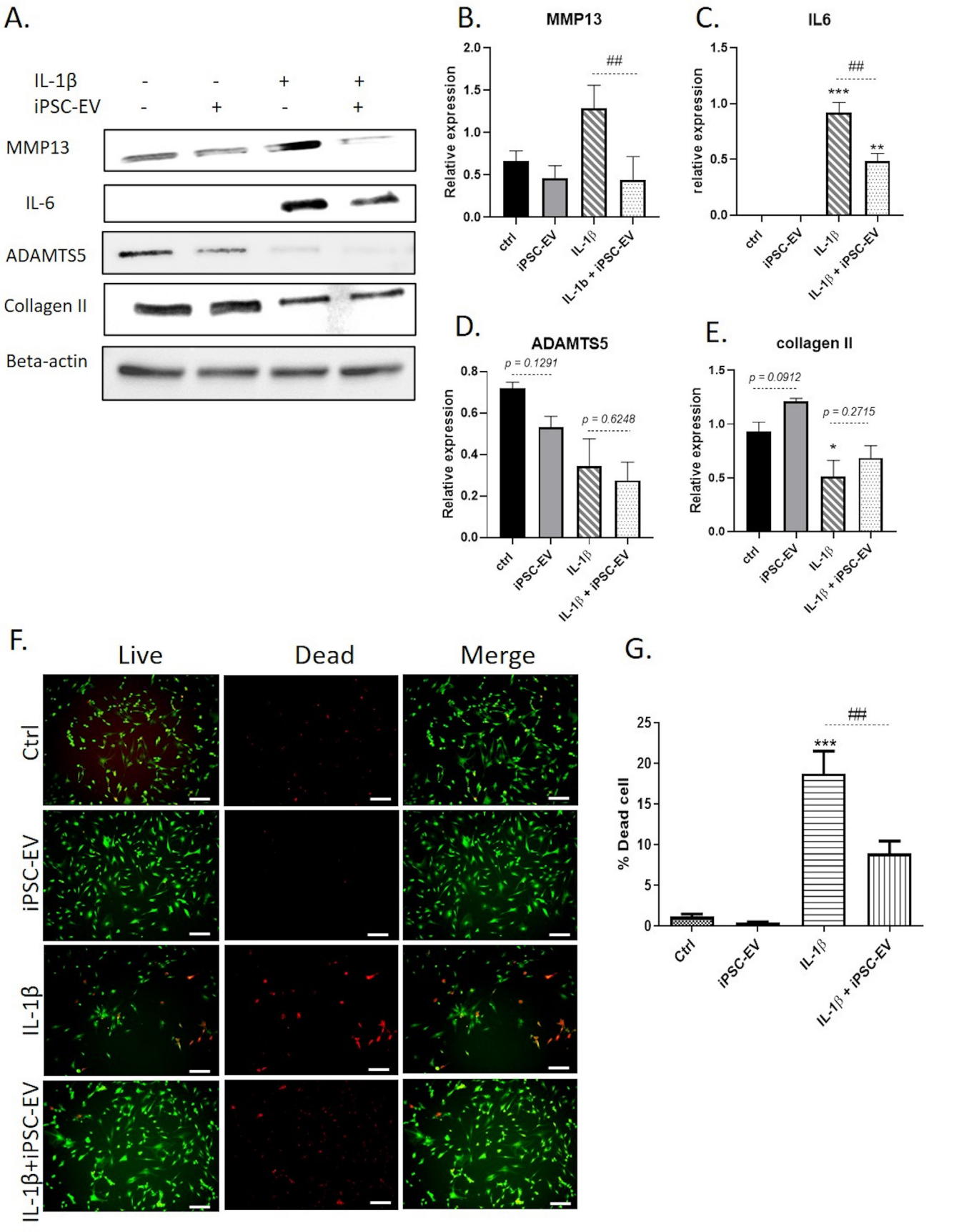

(caption on next page)

Figure 3. iPSC-EV alleviated IL-1β-induced inflammation and cell death of chondrocytes. A. Representative western blot image showing the expression level of MMP13, IL-6, ADAMTS5, and collagen II in chondrocytes stimulated with IL-1β and iPSC-EV. B.-E. Quantification of protein level from western blot analysis (n = 3) F. Live and dead cell labelling observed using a fluorescence microscope, after incubating the chondrocyte with IL-1β for 24 h. Scale bar = 200 μm. G. Quantification of the percentage of apoptotic chondrocytes in live and dead cell assays (n = 4) *Significant difference to control: *p < 0.05, **p < 0.01, ***p < 0.005. #Significant difference between groups: ##p < 0.01.
Abbreviations: iPSC-EV: induced pluripotent stem cell-derived extracellular vesicles; IL-1β: Interleukin 1 beta; MMP13: matrix metallopeptidase 13; IL-6: Interleukin 6; ADAMTS5: a disintegrin and metalloproteinase with thrombospondin motifs 5.

assay confirmed that cell proliferation of the chondrocytes was significantly enhanced ($p < 0.05$) by the iPSC-EV supplement (Fig. 2B).

The ageing or senescence of chondrocytes leads to an imbalance in homeostasis and loss of articular cartilage, a hallmark of OA [18]. We established an *in vitro* model of long-term low-dose H_2O_2 exposure to induce chondrocyte senescence (Fig. 2C). Long-term treatment with 10 μM of H_2O_2 induced cell senescence, as indicated by morphological changes and SA-β-galactosidase staining (Fig. 2D, E). Irregular-shaped cells with larger nuclei and cell bodies were mainly observed in the chondrocytes treated with H_2O_2. These cells were strongly positive for SA-β-galactosidase staining, indicating senescence with strong β-galactosidase activity (Fig. 2D). The percentage of positively stained cells significantly increased in the H_2O_2 treated group ($p < 0.01$) (Fig. 2E), and the number of stained cells significantly reduced in the H_2O_2+ iPSC-EVs group ($p < 0.05$) compared to the H_2O_2 group, indicating iPSC-EV treatment significantly alleviated H_2O_2-mediated senescence. We observed that the percentage of positive cells in the no-treatment group, which had a reduced number of iPSC-EVs ($p = 0.8836$), was low. Western blot analysis revealed that protein expression of senescence marker p21 was significantly induced by H_2O_2 treatment ($p < 0.01$), whereas iPSC-EV reduced its expression ($p < 0.05$) (Fig. 2F, G). Collagen II expression was also significantly reduced in senescent cells ($p < 0.05$). Treatment with iPSC-EV insignificantly enhanced collagen II expression in both normal and H_2O_2-induced senescent conditions (Fig. 2F, H). Therefore, iPSC-EVs have anti-ageing potential on H_2O_2-mediated cell senescence via p21 suppression.

3.3. iPSC-EV alleviated inflammation and cell death in IL-1β-inducedin vitro OA model

To investigate the therapeutic effect of iPSC-EVs on OA chondrocytes*in vitro*, IL-1β was used to induce chondrocyte damage. 10 ng/mL of IL-1β markedly stimulated the protein expression of the metalloprotease MMP-13 and cytokine IL-6 in chondrocytes (Fig. 3A). This effect was significantly attenuated after the administration of iPSC-EVs ($p < 0.01$) (Fig. 3B, C). IL-1β suppressed the expression of the aggrecanase ADAMTS5. However, iPSC-EV suppressed the expression of ADAMTS5 in both normal and IL-1β-treated conditions, though this was not statistically significant (Fig. 3A, D). Furthermore, the expression of collagen II by chondrocytes significantly decreased after treatment with IL-1β ($p < 0.05$). iPSC-EVs did not significantly enhance the expression of collagen type II in normal chondrocytes ($p = 0.0912$) or chondrocytes under the effect of IL-1β ($p = 0.2715$).

We examined the potential of iPSC-EVs in attenuating chondrocyte cell death. IL-1β (20 ng/mL) was applied to trigger chondrocyte cell death (Fig. 3F). Red fluorescence, representing dead cells, was high in intensity in the IL-1β treated group without iPSC-EVs. The quantification graph (Fig. 3G) shows that dead cells increased significantly in IL-1β treated chondrocytes ($p < 0.005$) and significantly reduced after iPSC-EV treatment ($p < 0.01$). This suggested that iPSC-EVs alleviated the IL-1β-mediated cell death of chondrocytes.

3.4. iPSC-EV modulated macrophage polarisation and inflammatory cytokine secretion

Synovial macrophages contribute to the progression of inflammation in OA. The abundance of M1 macrophages can mediate OA progression and pain [19]. Thus, targeting macrophage polarisation and activity is another option for OA treatment. Here, we explored the effect of iPSC-EVs on macrophage polarisation and cytokine secretion. PMA was applied to mediate the maturation of THP-1 monocytes to the naïve M0 state. LPS and IFN-γ induced pro-inflammatory M1 macrophage polarisation. iNOS and CD206 were used as M1 and M2 macrophages markers, respectively. LPS + IFN-γ administration skewed M0 toward M1 macrophages by significantly reducing CD206 and inducing iNOS expression ($p < 0.01$) (Fig. 4A–D). iPSC-EV treatment significantly enhanced CD206 expression in both naïve M0 and activated M1 macrophages ($p < 0.05$). iNOS expression was not significantly suppressed in M0 cells exposed to iPSC-EV ($M0^{EV+}$) compared to control M0 ($p = 0.4416$). Only subtle changes in iNOS were detected in M1 macrophages. TNF-α, another cytokine marker of M1, was significantly reduced in $M0^{EV+}$ compared to control M0 ($p < 0.05$). ELISA was used to evaluate the cytokine secretion by macrophages. We revealed that TNF-α, IL-6, and IL-1β were highly secreted by LPS + IFN-γ activated M1 macrophages. iPSC-EVs significantly depleted the secretion of $M0^{EV+}$ (Fig. 4E–G). Taken together, iPSC-EVs were able to induce $CD206^+$ macrophage polarisation and alter cytokine secretion.

3.5. iPSC-EV affected macrophage-chondrocyte interplay

We further investigated whether these altered macrophage phenotypes indirectly affected chondrocyte degradation. CMs from different phenotypes of macrophages were collected and applied to chondrocytes. We incubated the chondrocytes in 50% macrophage CM for 24 h. Protein expression was assessed by western blot analysis. Collagen II expression in chondrocytes was significantly abolished when cultured with M0 or M1 CM ($p < 0.001$) (Fig. 5A, B). In comparing chondrocyte + M0 CM and chondrocyte + $M0^{EV+}$ CM, collagen II expression of chondrocyte + $M0^{EV+}$ CM was significantly higher ($p < 0.01$). The macrophage CM did not increase ADAMTS5 expression in chondrocytes. However, its expression was not significantly lower in chondrocyte + $M0^{EV+}$ and $M1^{EV+}$ CM compared to chondrocyte + M0 and M1 CM, respectively (Fig. 5A, C). IL-6 expression was stimulated in chondrocyte + M0 CM and was alleviated in chondrocyte + $M0^{EV+}$ CM (Fig. 5A, D). IL-6 expression in chondrocytes treated with CM from M1 and $M1^{EV+}$ cells was extremely high. No difference was detected between the expression levels of both groups.

We co-cultured chondrocytes with macrophages of different phenotypes using Transwell assays. After 24 h of co-culture, the chondrocytes were subjected to double immunostaining for MMP13 and collagen II (Fig. 5E). MMP13 expression was not significantly enhanced in chondrocytes co-cultured with M0 or M1 (Fig. 5F). In contrast, collagen II expression was significantly depleted in M0 and M1 co-cultured groups. Interestingly, their altered expression was reversed in chondrocytes co-cultured with iPSC-EV-treated M0 and M1 ($M0^{EV+}$ co and $M1^{EV+}$ co) (Fig. 5G). Furthermore, the CM of chondrocytes after treatment was collected to observe the secretion of MMPs using an MMP array assay (Fig. 5H). Chondrocytes co-cultured with $M0^{EV+}$ secreted lower MMP3 and higher TIMP-1 levels than those exposed to M0 (Fig. 5I, J). Chondrocytes co-cultured with M1 secreted significantly higher MMP10 levels than those exposed to $M1^{EV+}$ (Fig. 5K). Therefore, iPSC-EVs probably indirectly ameliorate chondrocyte degradation by regulating macrophage polarisation and cytokine secretion, which interact with chondrocytes.

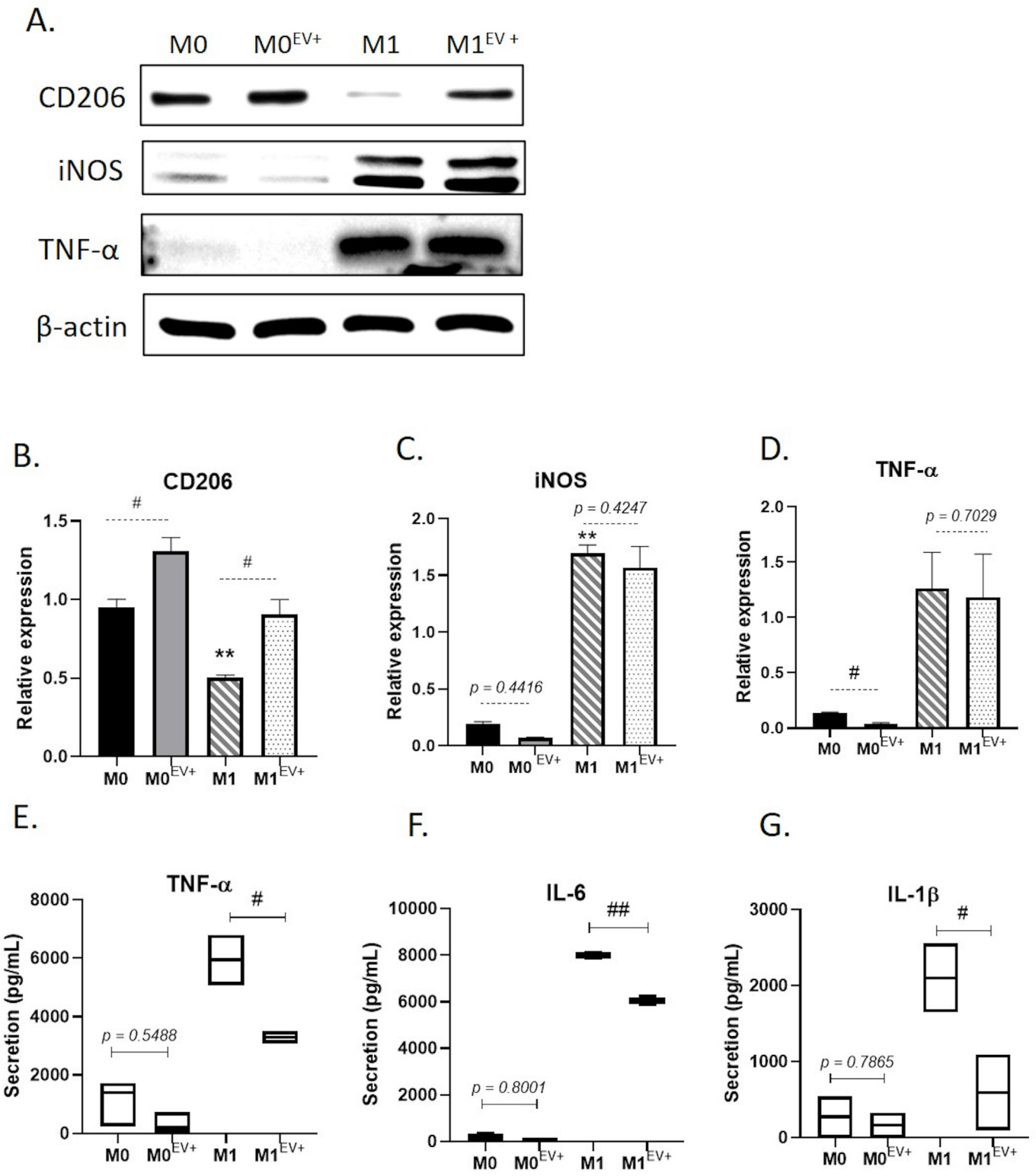

Figure 4. iPSC-EV regulated macrophage polarisation and cytokine secretion. A. Representative western blot image showing the expression of a M2 marker (CD206) and M1 markers (iNOS, and TNF-α) in M0, $M0^{EV+}$, M1, and $M1^{EV+}$. B.-D. Quantification of protein abundance from western blot results (n = 3) E-G. ELISA analysis of cytokines secreted by macrophages under different conditions (n = 3) *Significant difference to control: **$p < 0.01$. #Significant difference between groups: #$p < 0.05$, ##$p < 0.01$).

Abbreviations: PSC-EV: induced pluripotent stem cell-derived extracellular vesicles; IFN-γ: Interferon gamma; iNOS: inducible nitric oxide synthase; TNF-α: tumour necrosis factor alpha

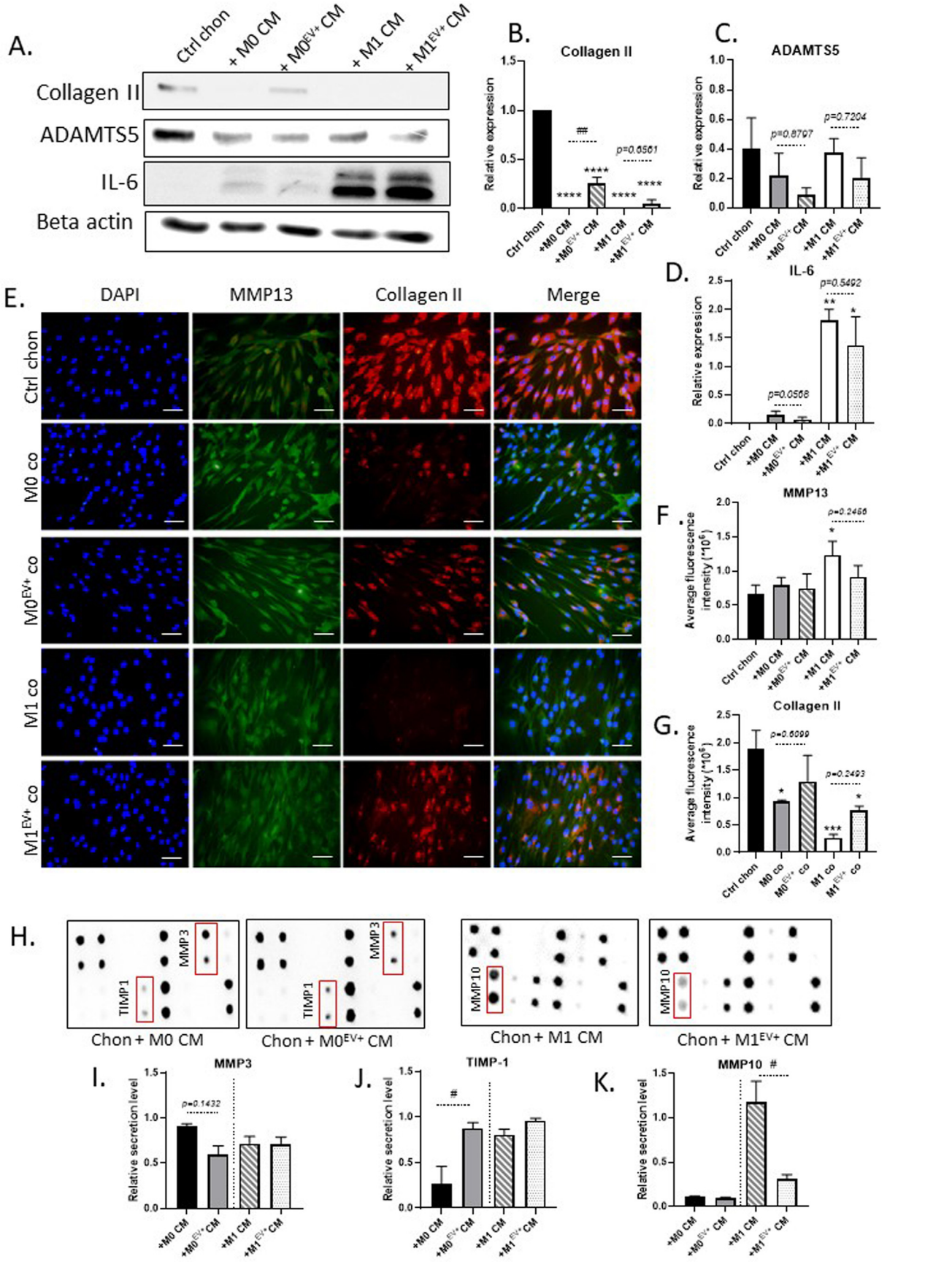

(caption on next page)

Figure 5. Effect of the microenvironment of iPSC-EV treated macrophages on the chondrocytes. A. Representative western blot image showing the proteins expressed by the chondrocytes treated with macrophage CM. B.-D. Densitometry of western blot analysis (n = 3) E. Immunofluorescence double staining of collagen II (red) and MMP13 (green) in chondrocytes co-cultured with different macrophages. Scale bar = 100 μm. F., G. Quantification of fluorescence signal intensity of collagen II and MMP13. H. MMP array analysis of the chondrocyte CM after incubating in different macrophage CMs. I.-K. Relative secretion levels of MMP3, MMP-10 and TIMP-1 from MMP array analysis. *Significant difference to control: *$p < 0.05$, **$p < 0.01$, ***$p < 0.005$, ****$p < 0.001$. #Significant difference between groups: #$p < 0.05$, ##$p < 0.01$. (For interpretation of the references to colour in this figure legend, the reader is referred to the Web version of this article.)
Abbreviations: iPSC-EV: induced pluripotent stem cell extracellular vesicles; MMP: matrix metallopeptidase; TIMP: tissue inhibitor of metalloproteinases

3.6. iPSC-EV alleviated inflammation and degradation of articular cartilage in ACLT rabbit

To validate the effect of iPSC-EVs in the *in vivo* OA model, we established an OA model in rabbits using the ACLT method. Three weeks after ACLT, iPSC-EVs or equal volumes of PBS were injected intra-articularly once a week. We observed the gross lesion before sample collection and demonstrated that ACLT caused severe damage to the articular cartilage, including bruising, surface protrusion, erosion, and redness, particularly to the ACLT group (Fig. 6A). Meanwhile, we found milder lesions with redness, bruising, and mild erosion in the ACLT + iPSC-EV group (Fig. 6A). The iPSC-EV group showed no signs of inflammation or damage. Histopathological analysis using HE (Fig. 6B) and toluidine blue stains (Fig. 6C) indicated that intact articular cartilage surface was found in the tissues of the normal and iPSC-EV groups. Severe articular surface abrasion, erosion, fibrillation, and extended fissures were found in all tissue samples of the ACLT group (Fig. 6B, C). Milder abrasion and erosion on the cartilage surface were observed in the ACLT + iPSC-EV group. Hypercellular clusters were detected in the lesion area of the ACLT tissue and ACLT + iPSC-EV (Fig. 6B). Subchondral bone sclerosis and subchondral cysts with fibrous tissue were found in the ACLT group (Fig. 6D). Furthermore, ACLT and ACLT + iPSC-EV tissue showed reduced safranin-O staining (Fig. 6D), indicating proteoglycan loss in the cartilage. The synovial membrane of each group was evaluated from HE staining (Fig. 6E). Severe hyperplasia and hypertrophy of synoviocytes were found in the ACLT group. Mild hyperplasia of synovium was also observed in the ACLT + iPSC-EV group. The Osteoarthritis Research Society International (OARSI) score was evaluated by an experienced pathologist. The average OARSI score in the ACLT group was significantly higher than that in the ACLT + iPSC-EV group ($p < 0.001$) (Fig. 6E). Thus, OA-like lesions using the ACLT model and iPSC-EV treatment protected the articular cartilage from severe OA lesion progression.

IHC was performed to evaluate the expression of degradation proteins in the cartilage chondrocytes. Collagen II, MMP13, ADAMTS5, and TNF-α expression were observed in the cartilages (Fig. 7). The expression of collagen II was dramatically reduced in the superficial to deep zones of the articular cartilage of the ACLT group, particularly in the lesion area. Collagen II expression in the superficial layer in ACLT + iPSC-EV was also reduced. ADAMATS5 expression was found in superficial layers of every group, including the iPSC-EV group, and was most enriched in the superficial to deep layers of the lesion area of the ACLT group. MMP13 and TNFα expression was enriched in the superficial to mid-layer of the ACLT articular cartilage. The ACLT + iPSC-EV-treated articular cartilage exhibited stronger collagen II and weaker MMP13, ADAMTS5, and TNFα than the ACLT group. Therefore, iPSC-EVs alleviate inflammation and degradation of chondrocytes by maintaining collagen II expression and suppressing MMP13, ADAMTS5, and TNFα expression during OA progression.

4. Discussion

iPSC-EVs have been previously reported for their effectiveness in cardiac repair [20] and the anti-ageing of skin fibroblasts and MSCs [21]. In this study, iPSC-EVs significantly stimulated the proliferation ability of chondrocytes. Chondrocytes play an essential role in cartilage maintenance through their metabolic turnover and synthesis of ECM components [22]. Thus, chondrocyte proliferation and metabolic homeostasis and function are the major factors involved in the repair of injured cartilage.

One of the predisposing causes of OA is chondrocyte senescence. Ageing chondrocytes lose their proliferation ability, homeostasis, and functions such as ECM synthesis and its response to growth factors and cytokines [23]. Several studies have demonstrated that the incubation of chondrocytes with H_2O_2 promotes the senescence-like phenotype of chondrocytes [24]. This study demonstrated that long-term treatment with low-dose H_2O_2 triggered cell senescence. Meanwhile, iPSC-EV administration ameliorated cell senescence by reducing p21 expression and maintaining collagen II expression. Price et al. [25] demonstrated that the presence of SA-β-galactosidase-positive cells in cartilage is predominantly associated with OA lesions. Furthermore, suppressing the expression of p21, a senescence marker, accelerates cartilage tissue repair [26]. Therefore, we assume that iPSC-EVs may have the potential to slow the progression of OA and accelerate cartilage regeneration. Similar anti-senescence effects of iPSC-EVs have been reported in senescent MSCs, including the reduction of SA-β-galactosidase enzymatic activity and expression of senescence proteins (p21, p53) [27]. To the best of our knowledge, this is the first study showing that iPSC-EVs have the potential to alleviate *in vitro* ageing of cartilage cells. An *in vivo* study of the effect of iPSC-EVs on age-related OA is also required.

We created an IL-1β-induced OA model *in vitro*. IL-1β treatment of chondrocytes is one of the most common *in vitro* OA models used in several studies [12]. These studies showed that IL-1β is an independent pro-inflammatory cytokine that stimulates inflammation and apoptosis and leads to OA progression. Our results consistently revealed that IL-1β significantly induced the expression of the matrix-degrading enzyme MMP13. IPSC-EVs significantly reversed this effect. An increase in the MMPs, ADAMTS family enzymes, and other important catabolic enzymes of chondrocytes, drive ECM degradation and cartilage destruction [28]. The expression of ADAMTS5 is usually aberrant in the early stages of OA [29]. Conversely, we found that ADAMTS5 expression was decreased after IL-1β treatment, consistent with a previous gene expression profile report of IL-1β treated chondrocytes [30].

In addition to its effect on anabolic-catabolic protein expression, IL-1 activates other mediators of synthesis in chondrocytes, such as IL-6, which downregulates collagen II and aggrecan [31]. We consistently demonstrated that IL-6 cytokine expression in chondrocytes significantly increased after IL-1β treatment, whereas collagen II expression significantly decreased. iPSC-EVs alleviated these effects to protect the chondrocytes. Furthermore, iPSC-EVs significantly attenuated IL-1β-mediated chondrocyte cell death. Therefore, iPSC-EVs can protect chondrocytes from IL-1β mediated inflammation, anabolic-catabolic imbalance, and cell death by regulating the catabolic enzymes MMP13 and IL-6 and supporting collagen II production.

In patients with OA, inflammation is commonly observed in chronic and lower grades. The imbalance of pro-inflammatory M1 and anti-inflammatory M2 macrophages is associated with the initiation, progression, and severity of OA [32]. OA synovium contains many $iNOS^+$ M1-like macrophages and a slightly lower number of $CD206^+$ macrophages than healthy synovium [33]. Activated M1 cytokines and the M1/M2 ratio are increased in OA synovium, leading to cartilage degradation and osteophyte formation [34]. Therefore, targeting inflammatory macrophages and related pathways may mitigate the severity and progression of OA. In this study, iPSC-EVs induced the expression of the M2 surface marker CD206 and suppressed that of iNOS, an M1 marker. iPSC-EVs also significantly reduced M1 macrophage secretory cytokines

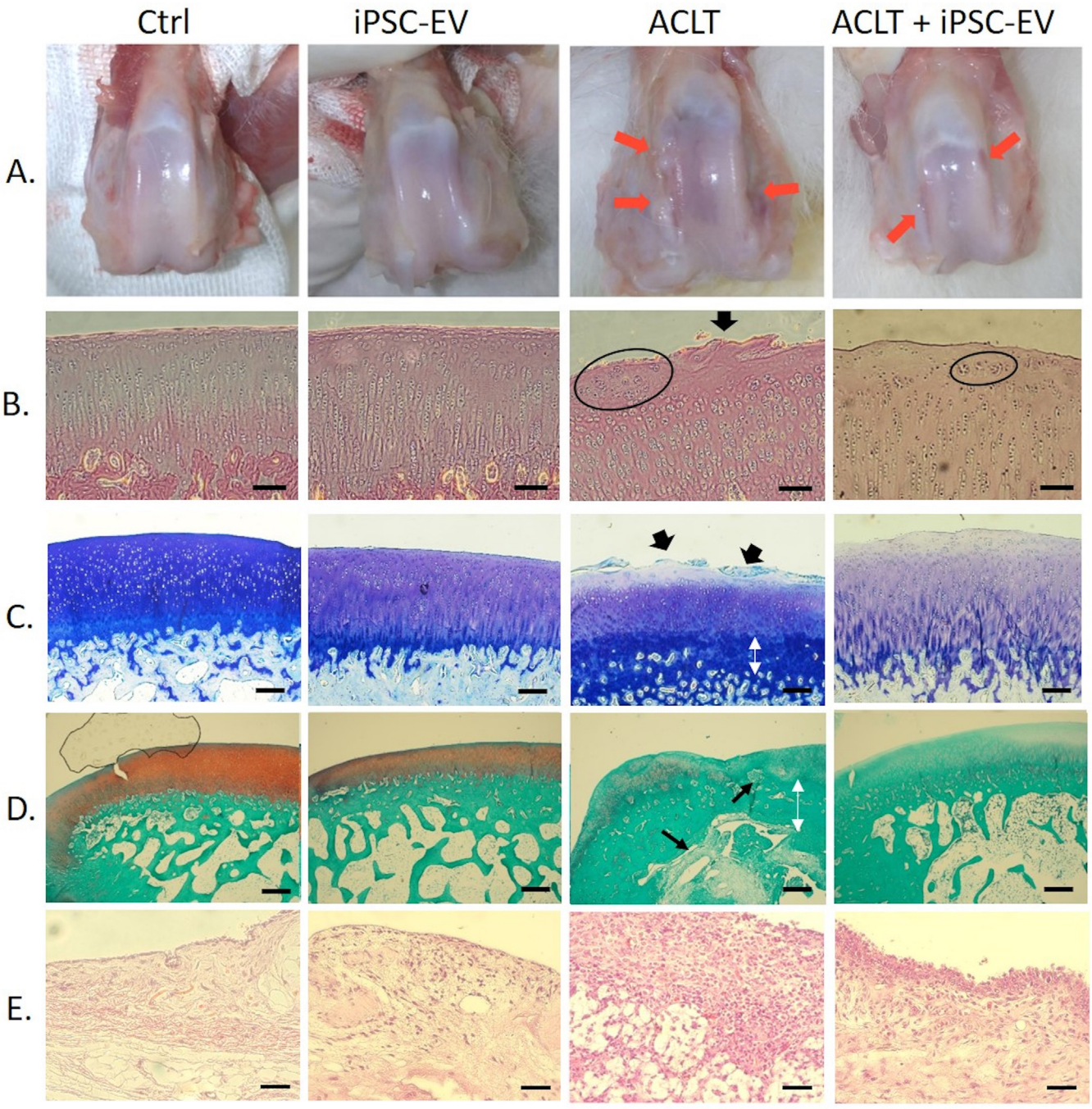

(caption on next page)

Figure 6. Gross lesion and histopathological study of rabbit articular cartilage after anterior cruciate ligament transection and iPSC-EV injection. A. Gross lesion showing the articular cartilage destruction including surface erosion, and protrusion (red arrows) in the rabbit that underwent ACLT. B. Haematoxylin eosin (20x), C. Toluidine blue (10x), and D. Safranin-O (4x) staining showing the pathological structure of the rabbit cartilage. Wide black arrows indicate areas of severe damage. Black ovals indicate hypercellular clusters. Narrow white arrows indicate subchondral bone sclerosis. Narrow black arrows indicate subchondral cysts with fibrous tissue (B. scale bar = 100 μm, C. and D. scale bar = 500 μm) E. Synovial membrane of each group (40X objective, scale bar = 50 μm) F. OARSI score of the samples (control n = 9, iPSC-EV n = 3, ACLT n = 3, ACLT + iPSC-EV n = 3) *Significant difference to control; ****p < 0.001. #Significant difference between groups; ####p < 0.001. (For interpretation of the references to colour in this figure legend, the reader is referred to the Web version of this article.)
Abbreviations: ACLT: Anterior cruciate ligament transection; PSC-EV: induced pluripotent stem cell-derived extracellular vesicles

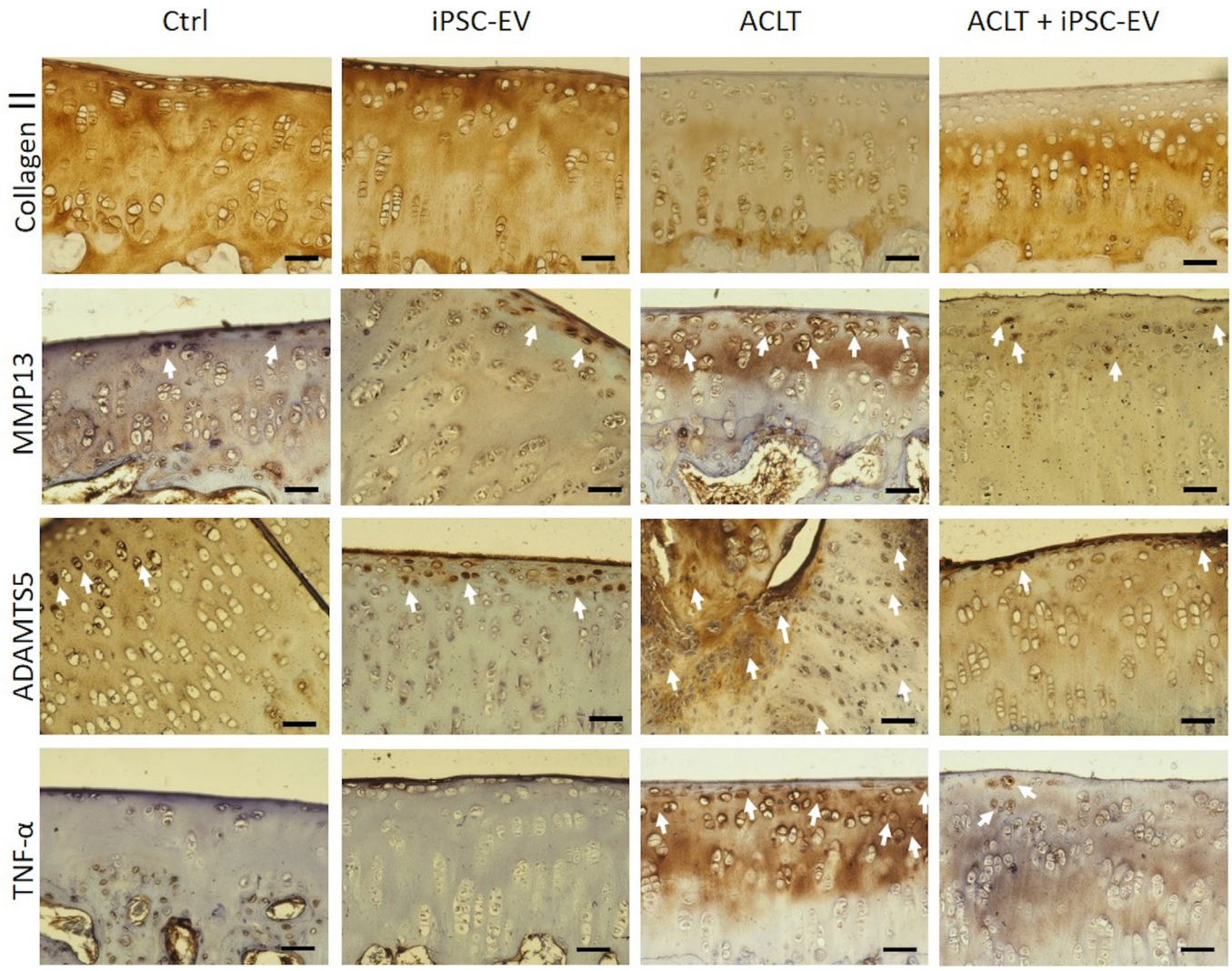

Figure 7. Immunohistochemical study showed the protein expression of collagen II, MMP13, ADAMTS5, and TNF-α in rabbit articular cartilage tissue from different treatments. White arrows indicate positive cells. Scale bar = 50 μm.

such as IL-1β, IL-6, and TNF-α, which may lead to the degradation of ECM matrix proteins and loss of proteoglycan and collagen [31]. Inhibiting TNF-α suppresses the expression of interleukins, MMPs, VEGF, and ADAMTS4 in rats with OA [35]. Thus, iPSC-EVs could modulate inflammation and progression of OA by affecting macrophage polarisation and cytokine production, such as TNF-α and interleukins.

Recently, several OA-related studies have discussed the paracrine interactions of macrophages and chondrocytes. Chondrocytes co-cultured with LPS-activated M1 macrophages significantly increased the expression of MMPs and inflammatory cytokines such as ILs, TNF-α, and IFN-γ. Chondrocytes also induced IL-1β and VEGF-A expression in macrophages [36]. Cartilage explants cultured with IFN-γ+TNF-α-induced macrophages could upregulate ILs, MMP13 and ADAMTS5 while inhibiting aggrecan and collagen II [37]. Fahy et al. [38] showed that CM of IFN-γ or LPS-activated M1 macrophages inhibited chondrocyte differentiation by decreasing aggrecan and collagen II. Thus, regulating synovial macrophage polarisation is another important factor in OA patients. In our study, iPSC-EVs reformed the phenotype of PMA-induced M0 and LPS + IFN-γ – induced M1 macrophages. This change in the inflammatory milieu thus interplayed with the chondrocytes. Chondrocytes exposed to iPSC-EV-treated macrophages, particularly in the M0 state, exhibited milder damage than those exposed to control macrophages. This result suggests that iPSC-EVs not only directly regulate the inflammatory response of chondrocytes but might also regulate synovial inflammatory macrophages.

The MMP array showed that chondrocytes in contact with the CM of iPSC-EV-treated M0 secreted lower levels of MMP3 and MMP8 and higher TIMP-1 compared with those in the M0 CM. TIMP is an

endogenous inhibitor of MMPs and ADAMTS. Balancing MMP and TIMP is necessary for cartilage homeostasis [39]. This result emphasised that iPSC-EV modified the macrophage microenvironment toward an anti-inflammatory mode and led the chondrocytes to milder inflammation and homeostatic loss through balancing between collagen II and catabolic enzyme MMPs. Although iPSC-EVs significantly modulated cytokine secretion by M1 macrophages, the effect of M1 and $M1^{EV+}$ microenvironments on chondrocytes was insignificant. The concentration of inflammatory cytokines secreted from M1 may have been harmful to the chondrocytes. Thus, chondrocytes exposed to 50% M1 and $M1^{EV+}$ CM were severely damaged.

Finally, we validated iPSC-EVs' therapeutic benefit in an ACLT-mediated OA rabbit model. ACLT is one of the most common methods of inducing post-traumatic OA (PTOA), causing joint destabilisation and degeneration of articular cartilage [40]. In this study, ACLT caused PTOA in all the rabbits; the severity was ameliorated by intra-articular injection of iPSC-EVs. Consistent with the *in vitro* study, iPSC-EV injection reduced the inflammation and degeneration of articular cartilages. The gross lesion on the articular surface, subchondral bone and synovium of the ACLT was prominent, whereas the lesion on the articular surface of the iPSC-EV treated groups was milder. IHC also emphasised that iPSC-EV reduced cartilage degeneration by suppressing MMP13 and ADAMTS5 expression by the chondrocytes. Although the IL-1β did not stimulate ADAMTS5 expression in chondrocytes *in vitro*, ACLT induced MMP13, TNFα and ADAMTS5 expression *in vivo*. Our *in vitro* IL-1β experiment included short duration (24 h incubation) treatment, while the *in vivo* ACLT model had a more extended period (over one month) of stress. Therefore, the different stress and duration probably caused different expression patterns of ADAMTS5. However, we found that iPSC-EVs attenuated ADAMTS5 expression in ACLT rabbit cartilage. Wang et al. [11] showed that ESC-MSC-derived exosomes alleviated cartilage destruction and matrix degradation by increasing collagen II and decreasing ADAMTS5 in the destabilisation of the medial meniscus model of mice. Therefore, iPSC-EVs have therapeutic benefits for OA in rabbit model.

In our study, the iPSC was cultured in serum-free medium before EV harvesting to avoid contamination of external EVs. Similar to the report of Cavallo et al. [15], non EV-depleted FBS was used in target cell (THP-1 and chondrocyte) culturing. Though the control and EV-treated target cells were cultured in the same prepared media, we reduced the FBS concentration (1% or 5%, for chondrocytes and macrophages, respectively), to minimize the effect of serum EV. The reduced FBS concentration may have affected the differences from 10% FBS.

In conclusion, iPSC-EVs ameliorated OA by enhancing collagen II synthesis, suppressing matrix degradation enzymes such as MMPs and ADAMTS5, and reducing inflammation. The anti-inflammatory effect of iPSC-EVs was determined by the direct regulation of chondrocytes or the indirect regulation of macrophages. iPSC-EVs stimulated the proliferation and alleviated the senescence of chondrocytes by downregulating p21 and upregulating collagen II expression. In the rabbit ACLT-induced OA model, iPSC-EV injection reduced cartilage degeneration, as indicated by the milder destruction, upregulation of collagen II and downregulation of MMP13, ADAMTS5, and TNF-α. Overall, our results suggest that iPSC-EVs possess therapeutic potential for OA treatment.

Author contributions

Yu-Huan Hsueh: Project administration, Writing - original draft **Waradee Buddhakosai:** Data curation, Project administration, Writing - review & editing, **Phung Ngan Le:** Methodology, Data curation, **Yung-Yi Tu:** Methodology, Data curation **Hsien-Chang Huang:** Methodology, Data curation **Huai-En Lu:** Conceptualization, Resources, Writing - review & editing **Wen-Liang Chen:** Conceptualization, Resources, Supervision **Yuan-Kun Tu:** Conceptualization, Supervision, Writing - review & editing.

Funding

The study was supported by the grants from the Ministry of Science and Technology (MOST) of the Taiwan Government (MOST 109-2314-B-650-002-MY2; MOST 109-2221-E-650-001-MY2; MOST 110-2224-E-080-001-MY2). The funding agency had no role in study design; in the collection, analysis and interpretation of data; in the writing of the report; and in the decision to submit the article for publication.

Declaration of competing interest

The authors have no conflicts of interest relevant to this article.

Acknowledgement

We greatly appreciate MASTER LABORATORY Co., Ltd for technical support of animal study.

Appendix A. Supplementary data

Supplementary data to this article can be found online at https://doi.org/10.1016/j.jot.2022.10.004.

References

[1] Cui A, Li H, Wang D, Zhong J, Chen Y, Lu H. Global, regional prevalence, incidence and risk factors of knee osteoarthritis in population-based studies. EClinicalmedicine 2020;29(30):100587. https://doi.org/10.1016/j.eclinm.2020.100587.
[2] Zhang Y, Jordan JM. Epidemiology of osteoarthritis. Clin Geriatr Med 2010;26:355–69. https://doi.org/10.1016/j.cger.2010.03.001.
[3] Man GS, Mologhianu G. Osteoarthritis pathogenesis – a complex process that involves the entire joint. J Med Life 2014;7:37–41.
[4] Martel-Pelletier J. Pathophysiology of osteoarthritis. Osteoarthritis Cartilage 1999;7:371–3. https://doi.org./10.1053/joca.1998.0214.
[5] Goldring MB, Otero M, Plumb DA, Dragomir C, Favero M, El Hachem K, et al. Roles of inflammatory and anabolic cytokines in cartilage metabolism: signals and multiple effectors converge upon MMP-13 regulation in osteoarthritis. Eur Cell Mater 2011;21:202–20. https://doi.org/10.22203/ecm.v021a16.
[6] Zhang W, Moskowitz RW, Nuki G, Abramson S, Altman RD, Arden N, et al. OARSI recommendations for the management of hip and knee osteoarthritis, Part II: OARSI evidence-based, expert consensus guidelines. Osteoarthritis Cartilage 2008;16:137–62. https://doi.org/10.1016/j.joca.2007.12.013.
[7] Grässel S, Muschter D. Recent advances in the treatment of osteoarthritis. 2020. p. F1000. https://doi.org/10.12688/f1000research.22115.1. F1000Res.
[8] Wakitani S, Imoto K, Yamamoto T, Saito M, Murata N, Yoneda M. Human autologous culture expanded bone marrow mesenchymal cell transplantation for repair of cartilage defects in osteoarthritic knees. Osteoarthritis Cartilage 2002;10:199–206. https://doi.org/10.1053/joca.2001.0504.
[9] Pers YM, Rackwitz L, Ferreira R, Pullig O, Delfour C, Barry F, et al. Adipose mesenchymal stromal cell-based therapy for severe osteoarthritis of the knee: A phase I dose-escalation trial. Stem Cells Transl Med 2016;5:847–56. https://doi.org/10.5966/sctm.2015-0245.
[10] Yang D, Wang W, Li L, Peng Y, Chen P, Huang H, et al. The relative contribution of paracrine effect versus direct differentiation on adipose-derived stem cell transplantation mediated cardiac repair. PLoS One 2013;8:e59020. https://doi.org/10.1371/journal.pone.0059020.
[11] Wang Y, Yu D, Liu Z, Zhou F, Dai J, Wu B, et al. Exosomes from embryonic mesenchymal stem cells alleviate osteoarthritis through balancing synthesis and degradation of cartilage extracellular matrix. Stem Cell Res Ther 2017;8:189. https://doi.org/10.1186/s13287-017-0632-0.
[12] Li S, Stöckl S, Lukas C, Götz J, Herrmann M, Federlin M, et al. hBMSC-derived extracellular vesicles attenuate IL-1β-induced catabolic effects on OA-chondrocytes by regulating pro-inflammatory signaling pathways. Front Bioeng Biotechnol 2020;8:603598. https://doi.org/10.3389/fbioe.2020.603598.
[13] Kim Y, Rim YA, Yi H, Park N, Park S-H, Ju JH. The generation of human induced pluripotent stem cells from blood cells: an efficient protocol using serial plating of reprogrammed cells by centrifugation. Stem Cell Int 2016;2016:1329459. https://doi.org/10.1155/2016/1329459.
[14] Liu S, Mahairaki V, Bai H, Ding Z, Li J, Witwer KW, et al. Highly purified human extracellular vesicles produced by stem cells alleviate aging cellular phenotypes of senescent human cells. Stem Cells (Dayton) 2019;37:779–90. https://doi.org/10.1002/stem.2996.
[15] Cavallo C, Merli G, Borzì RM, Zini N, D'Adamo S, Guescini M, et al. Small Extracellular Vesicles from adipose derived stromal cells significantly attenuate in vitro the NF-κB dependent inflammatory/catabolic environment of osteoarthritis. Sci Rep 2021;11:1053. https://doi.org/10.1038/s41598-020-80032-7.

[16] Hosseinkhani B, Kuypers S, van den Akker NMS, Molin DGM, Michiels L. Extracellular vesicles work as a functional inflammatory mediator between vascular endothelial cells and immune cells. Front Immunol 2018;9. https://doi.org/10.3389/fimmu.2018.01789.
[17] Schmitz N, Laverty S, Kraus VB, Aigner T. Basic methods in histopathology of joint tissues. Osteoarthritis Cartilage 2010;18(Suppl 3). https://doi.org/10.1016/j.joca.2010.05.026. S113–6.
[18] Loeser RF. Aging and osteoarthritis: the role of chondrocyte senescence and aging changes in the cartilage matrix. Osteoarthritis Cartilage 2009;17:971–9. https://doi.org/10.1016/j.joca.2009.03.002.
[19] Daghestani HN, Pieper CF, Kraus VB. Soluble macrophage biomarkers indicate inflammatory phenotypes in patients with knee osteoarthritis. Arthritis Rheumatol 2015;67:956–65. https://doi.org/10.1002/art.39006.
[20] Adamiak M, Cheng G, Bobis-Wozowicz S, Zhao L, Kedracka-Krok S, Samanta A, et al. Induced pluripotent stem cell (iPSC)-derived extracellular vesicles are safer and more effective for cardiac repair than iPSCs. Circ Res 2018;122:296–309. https://doi.org/10.1161/CIRCRESAHA.117.311769.
[21] Liu S, Mahairaki V, Bai H, Ding Z, Li J, Witwer KW, et al. Highly purified human extracellular vesicles produced by stem cells alleviate aging cellular phenotypes of senescent human cells. Stem Cell 2019;37:779–90. https://doi.org/10.1002/stem.2996.
[22] Archer CW, Francis-West P. The chondrocyte. Int J Biochem Cell Biol 2003;35:401–4. https://doi.org/10.1016/s1357-2725(02)00301-1.
[23] Loeser RF, Shanker G, Carlson CS, Gardin JF, Shelton BJ, Sonntag WE. Reduction in the chondrocyte response to insulin-like growth factor 1 in aging and osteoarthritis: studies in a non-human primate model of naturally occurring disease. Arthritis Rheum 2000;43:2110–20. https://doi.org/10.1002/1529-0131. 200009)43:9<2110::AID-ANR23>3.0.CO;2-U.
[24] Brandl A, Hartmann A, Bechmann V, Graf B, Nerlich M, Angele P. Oxidative stress induces senescence in chondrocytes. J Orthop Res 2011;29:1114–20. https://doi.org/10.1002/jor.21348.
[25] Price JS, Waters JG, Darrah C, Pennington C, Edwards DR, Donell ST, et al. The role of chondrocyte senescence in osteoarthritis. Aging Cell 2002;1:57–65. https://doi.org/10.1046/j.1474-9728.2002.00008.x.
[26] Ibaraki K, Hayashi S, Kanzaki N, Hashimoto S, Kihara S, Haneda M, et al. Deletion of p21 expression accelerates cartilage tissue repair via chondrocyte proliferation. Mol Med Rep 2020;21:2236–42. https://doi.org/10.3892/mmr.2020.11028.
[27] Oh M, Lee J, Kim YJ, Rhee WJ, Park JH. Exosomes derived from human induced pluripotent stem cells ameliorate the aging of skin fibroblasts. Int J Mol Sci 2018;19:1715. https://doi.org/10.3390/ijms19061715.
[28] Heinegård D, Saxne T. The role of the cartilage matrix in osteoarthritis. Nat Rev Rheumatol 2011;7:50–6. https://doi.org/10.1038/nrrheum.2010.198.
[29] Verma P, Dalal K. ADAMTS-4 and ADAMTS-5: key enzymes in osteoarthritis. J Cell Biochem 2011;112:3507–14. https://doi.org/10.1002/jcb.23298.
[30] Sandell LJ, Xing X, Franz C, Davies S, Chang LW, Patra D. Exuberant expression of chemokine genes by adult human articular chondrocytes in response to IL-1beta. Osteoarthritis Cartilage 2008;16:1560–71. https://doi.org/10.1016/j.joca.2008.04.027.
[31] Legendre F, Dudhia J, Pujol JP, Bogdanowicz P. JAK/STAT but not ERK1/ERK2 pathway mediates interleukin (IL)-6/soluble IL-6R down-regulation of type II collagen, aggrecan core, and link protein transcription in articular chondrocytes. Association with a down-regulation of SOX9 expression. J Biol Chem 2003;278:2903–12. https://doi.org/10.1074/jbc.M110773200.
[32] Liu B, Zhang M, Zhao J, Zheng M, Yang H. Imbalance of M1/M2 macrophages is linked to severity level of knee osteoarthritis. Exp Ther Med 2018;16:5009–14. https://doi.org/10.3892/etm.2018.6852.
[33] Zhang H, Lin C, Zeng C, Wang Z, Wang H, Lu J, et al. Synovial macrophage M1 polarisation exacerbates experimental osteoarthritis partially through R-spondin-2. Ann Rheum Dis 2018;77:1524–34. https://doi.org/10.1136/annrheumdis-2018-213450.
[34] Blom AB, van Lent PL, Libregts S, Holthuysen AE, van der Kraan PM, van Rooijen N, et al. Crucial role of macrophages in matrix metalloproteinase-mediated cartilage destruction during experimental osteoarthritis: involvement of matrix metalloproteinase 3. Arthritis Rheum 2007;56:147–57. https://doi.org/10.1002/art.22337.
[35] Li H, Xie S, Qi Y, Li H, Zhang R, Lian Y. TNF-α increases the expression of inflammatory factors in synovial fibroblasts by inhibiting the PI3K/AKT pathway in a rat model of monosodium iodoacetate-induced osteoarthritis. Exp Ther Med 2018;16:4737–44. https://doi.org/10.3892/etm.2018.6770.
[36] Samavedi S, Diaz-Rodriguez P, Erndt-Marino JD, Hahn MS. A Three-dimensional chondrocyte-macrophage coculture system to probe inflammation in experimental osteoarthritis. Tissue Eng 2017;23:101–14. https://doi.org/10.1089/ten.TEA.2016.0007.
[37] Utomo L, Bastiaansen-Jenniskens YM, Verhaar JA, van Osch GJ. Cartilage inflammation and degeneration is enhanced by pro-inflammatory (M1) macrophages in vitro, but not inhibited directly by anti-inflammatory (M2) macrophages. Osteoarthritis Cartilage 2016;24:2162–70. https://doi.org/10.1016/j.joca.2016.07.018.
[38] Fahy N, de Vries-van Melle ML, Lehmann J, Wei W, Grotenhuis N, Farrell E, et al. Human osteoarthritic synovium impacts chondrogenic differentiation of mesenchymal stem cells via macrophage polarisation state. Osteoarthritis Cartilage 2014;22:1167–75. https://doi.org/10.1016/j.joca.2014.05.021.
[39] Baker AH, Edwards DR, Murphy G. Metalloproteinase inhibitors: biological actions and therapeutic opportunities. J Cell Sci 2002;115:3719–27. https://doi.org/10.1242/jcs.00063.
[40] McCoy AM. Animal models of osteoarthritis: comparisons and key considerations. Vet Pathol 2015;52:803–18. https://doi.org/10.1177/0300985815588611.